Available online at www.sciencedirect.com

ScienceDirect

journal homepage: www.elsevier.com/locate/he

Adsorption kinetics of methane reformer off-gases on aluminum based metal-organic framework

Deniz Angi, Fehime Cakicioglu-Ozkan *

Izmir Institute of Technology, Chemical Engineering Department, Gulbahçe, Urla-İzmir, 35430, Turkey

HIGHLIGHTS

- The narrow and large pore from MIL- 53 (Al) was synthesized with the solvothermal method.
- Adsorption of CO_2, CO, H_2 and CH_4 gases were controlled with electrostatic interaction.
- Pore Diffusion were measured by using the ZLC method.
- The low values of heat of adsorption demonstrated that process is reversible.

GRAPHICAL ABSTRACT

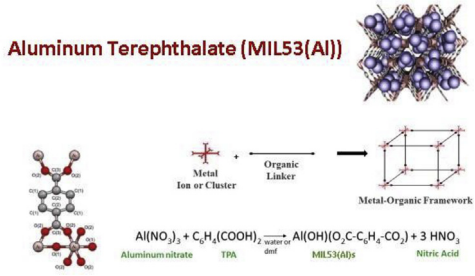

ARTICLE INFO

Article history:
Received 31 October 2019
Received in revised form
7 August 2020
Accepted 10 August 2020
Available online 10 September 2020

Keywords:
Adsorption
Hydrogen
Diffusion
MOF

ABSTRACT

Solvothermal synthesis of aluminum based metal-organic frameworks (MIL-53(Al)s) were conducted by considering the effects of crystallization and activation temperatures, and the solvent at purification step. Adsorption kinetics of Steam Methane Reformer off gas components at 34, 70 and 100 °C temperatures was measured by using ZLC method. Henry constant decreases as diffusion coefficient of the gases increases with increasing temperature; It was determined that the CO gas has the highest activation energy. Adsorption kinetics of gases were controlled with electrostatic interaction.

* *Corresponding author.*
E-mail addresses: fehimeozkan@iyte.edu.tr, fehimeozkan@yahoo.com (F. Cakicioglu-Ozkan).
https://doi.org/10.1016/j.ijhydene.2020.08.100

Introduction

CO_2 level of the earth is increased significantly after 1850 due to industrialization and fossil fuel usage and reached 408.64 ppm in 2019. This leads to global warming and climate change. Significant efforts are being made to create alternative clean and renewable energy sources to reduce environmental concerns and stress on the depletion of oil reserves. Although hydrogen is an ideal source of clean energy, high purity hydrogen is needed. This clean energy can be achieved by purifying the hydrogen-rich steam methane reformer (SMR) off gas consisting of 60–80% H_2, 15–25% CO_2, 3–6% CH_4 and 1–3% CO. Increasing demand for high purity gases has increased interest in commercial applications based on adsorption technologies for gas separation requiring less energy consumption and high efficiency [1,2]. The design and operation of this process involves profoundly understanding of the equilibrium and diffusion of the SMR-off gas components. Porous adsorbents possessing high selectivity and adsorption capacity are the key factors for an efficient design of the application of gas separation [3].

Metal-organic frameworks (MOFs), which have one (1D), two (2D) and three (3D) dimensional network structures, are coordination polymers consisting of organic linkers and inorganic metal clusters [4]. In addition to the inorganic and organic properties, the adjustable pore size and extremely high surface area (>1600 m^2/g) show that MOFs perform uniquely in adsorption based applications such as gas storage, gas cleaning, catalyst, and chemical sensor [5–10]. In MIL-53, aluminum is used as a metal and terephthalic acid as a ligand can be widely used in gas separation/purification applications due to its reversible breathing properties. Depending on the synthesis methods and parameters narrow-pore (np) form and/or large-pore (lp) form MIL-53(Al) was obtained by Mounfield et al. Liu et at [11–15]. The MIL-53(Al) structure is shown in Fig. 1.

In this study, aluminum based metal-organic frameworks (MIL-53(Al)) were synthesized considering the crystallization, activation temperature and the solvent in purification step via solvothermal method. Adsorption kinetics of SMR off-gas components was measured by using the ZLC technique.

Theory

The Zero Length Column (ZLC) method is a chromatographic technique proposed by Eic and Ruthven to measure the intracrystalline diffusion of gases in an adsorbent [16]. Under isothermal conditions without any adherence on the spherical adsorbent surface at high flow rate and low adsorbate concentration, differential mass transfer equation in ZLC is given by

$$V_s\frac{d\overline{q}}{dt}+V_g\frac{dC}{dt}+FC=0 \quad (1)$$

where V_g and V_s are present the volume of adsorptive and adsorbent, respectively. F is the volumetric flow rate. $\overline{q}$ and C are the average adsorbate and the adsorptive concentrations [17]. The dynamic behavior of an isothermal system of uniform spherical particles with linear equilibrium between the adsorbed and fluid phase can be described by;

$$\frac{\partial q}{\partial t}=D_c\left(\frac{\partial^2 q}{\partial r^2}+\frac{2}{r}\frac{\partial q}{\partial r}\right) \quad (2)$$

where r is the radius of the sphere, D_c is the intracrystalline diffusivity and q is adsorbed amount which is changed with time (t) and radial position (r). Considering the initial (Eq. (3)) and boundary conditions (Eq. (4)) and linear adsorption isotherm (Eq. (5)),

$$q=q_0\,,\ C=C_0 \quad \text{at} \quad t=0 \quad (3)$$

$$\left(\frac{\partial q}{\partial r}\right)_{r=o}=0 \quad \text{at} \quad t\neq 0 \quad (4)$$

$$q=KC \quad (5)$$

The analytical solution of Eqs. (1) and (2) gives the desorption curve (the ZLC response curve)

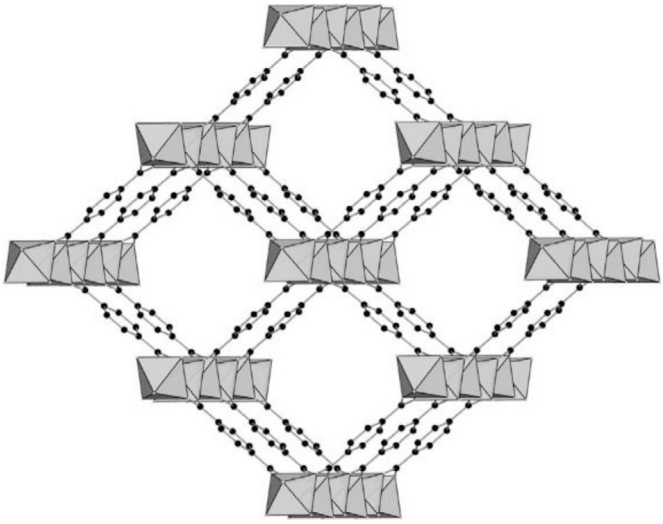

Fig. 1 – Framework structure of MIL53(Al) [4].

$$\frac{C}{C_o} = 2L\sum_{n=1}^{\infty} \frac{\exp\left(-\frac{\beta_n D_c t}{R_p^2}\right)}{\left[\beta_n^2 + L(L-1)\right]} \quad (6)$$

where β_n is the positive roots of the transcendental equation;

$$\beta_n \cot\beta_n + L - 1 = 0 \quad (7)$$

and

$$L = \frac{F}{3KV_s}\frac{R_p^2}{D_c} \quad (8)$$

In which R_p and K are the radius of the particle and the dimensionless Henry's Law constant [18]. If the L parameter is high enough (L > 10), mass transfer in the ZLC is controlled by diffusion. In this case, Eq. (6) can be simplified;

$$\ln\left(\frac{c}{c_0}\right) \approx \ln\left[\frac{2L}{\beta_1^2 + L(L-1)}\right] - \beta_1^2\frac{D_c t}{R_p^2} \quad (9)$$

where β_1 closes to π ($\beta_1 \rightarrow \pi$) and from plot of ln (C/Co) vs. t and L, Dc and K can be calculated using the long time region of the ZLC response curve [19].

Experimental

Materials and methods

In the synthesis of aluminum based metal-organic frameworks (MIL-53(Al)s), aluminum nitrate nonahydrate ($Al(NO_3)_3.9H_2O$, >99.5%), N,N-dimethylformamide ($(CH_3)_2$-NCOH, >99.8%, DMF hereafter) and methanol (CH_3OH,>99.9%, MetOH hereafter) were used as obtained impurities. Terephthalic acid (C_6H_4-1,4-$(CO_2H)_2$, BDC hereafter) was kindly supplied by PETKİM with high purity.

Synthesis of aluminum based metal-organic frameworks (MIL-53(Al)s)

MIL-53(Al) synthesis consisting of crystallization, purification and activation steps conducted under solvothermal conditions. Briefly the starting materials ($Al(NO_3)_3 \cdot 9H_2O$:BDC:DMF) with molar ratio of 1:1.48:184.5 were stirred at 330 rpm for 24 h at room temperature. The mixture was loaded into a Teflon-lined stainless steel autoclave and heated to crystallization temperature (Tc). At the end of the crystallization step, the solution was centrifuged at 3000 rpm for 25 min and the filtered product was suspended in DMF solution (50 mL) to start the purification step. The solution was heated to 130 °C for 24 h, and then centrifuged. This repeated two times to eliminate unreacted BDC remaining in the pores of the structure. Then, the structure was washed with MetOH with Soxhlet extraction for 20 h before the activation step. Finally, the MIL-53(Al)s were activated at 130 °C (200 °C or 330 °C) for 72 h to vaporize the remaining trace amount of impurities from the structure.

Characterization of MIL-53(Al)s

The morphologies and crystallographic structure of the synthesized MIL-53(Al)s were evaluated by scanning electron microscope (SEM, FEI QUANTA 250 FEG) and X-ray diffraction (XRD, Philips X' Pert Pro Diffractometer) with a standard scan speed of 2°/min and a step size of 0.002° under CuKα radiation. Thermal stability and the impurities were investigated by Thermogravimetric analysis (Shimadzu, TGA-51) with the heating rate of 10 °C/min under dry air flow rate of 40 mL/min. Interaction between atoms presented in the structure of MIL-53(Al)s were examined by Fourier Transform Infrared spectrophotometer (FTIR, Shimadzu 8201) requiring preparation of the pellets consisting of MIL-53 sample (1.5 mg) and KBr

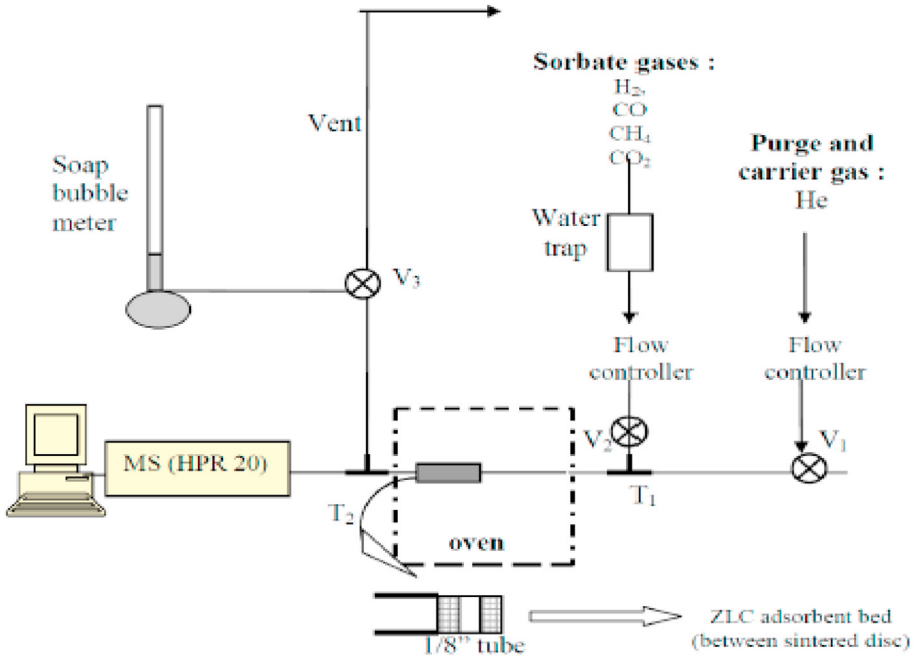

Fig. 2 – Experimental set-up of ZLC system.

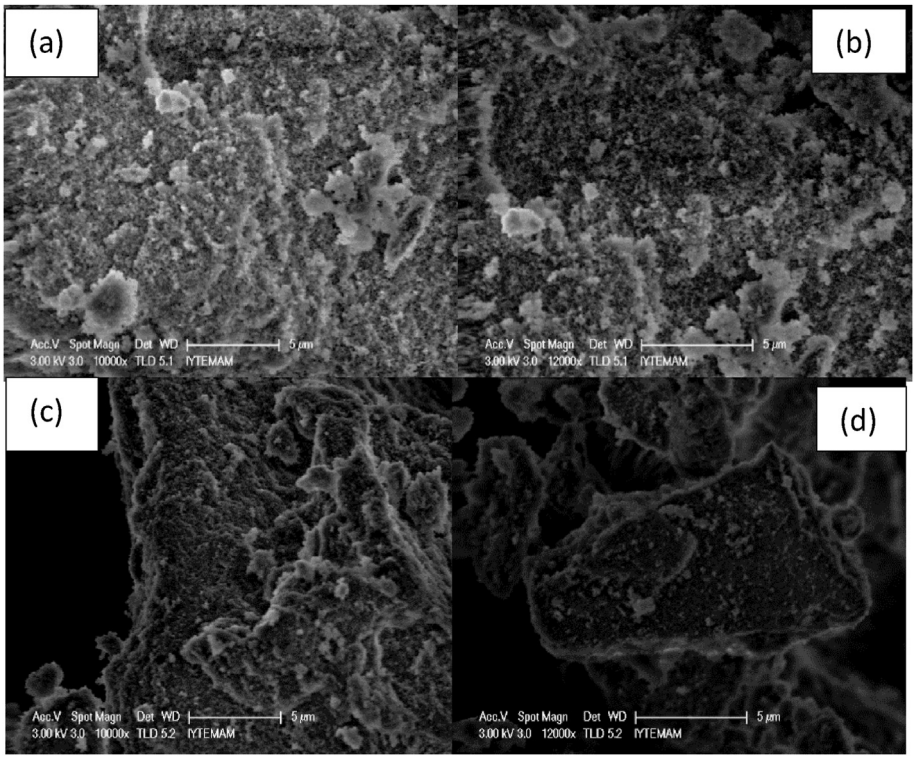

Fig. 3 – The SEM images (a) MIL53(Al)$_{S2}$ (b) MIL53(Al)$_{S3}$ (c) MIL53(Al)$_{S4}$ and MIL53(Al)$_{S5}$.

(148.5 mg). Textural properties were investigated performing N_2 adsorption isotherms at 77.35 K by using volumetric adsorption instrument (Micromeritics ASAP 2010 M) after degassing at 200 °C for 24 h under vacuum.

Adsorption kinetic studies

Adsorption kinetics of CO_2, CH_4, H_2 and CO gases on synthesized MIL-53(Al) was measured in a home-made ZLC system. Simplified schematic diagram of the ZLC experimental system

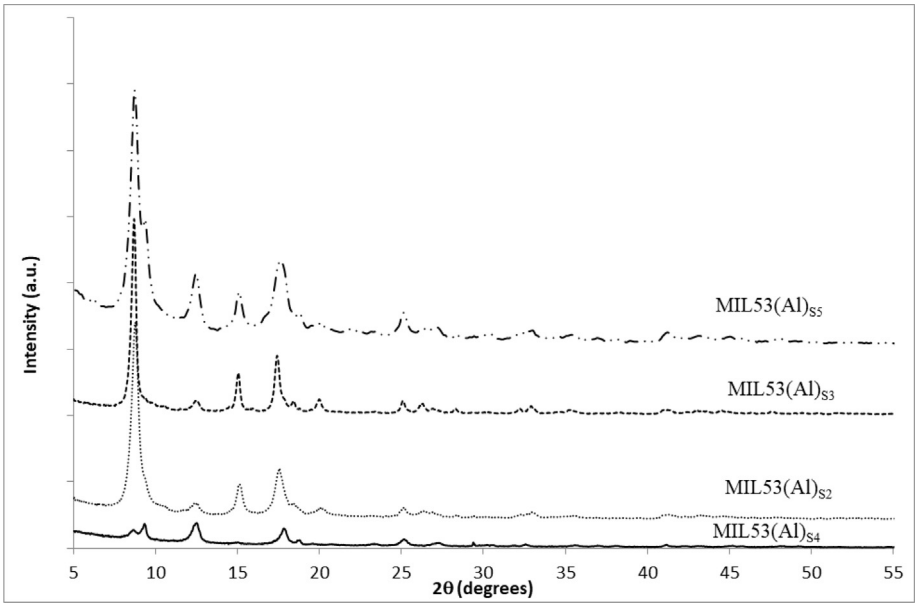

Fig. 4 – XRD patterns of MIL53(Al)$_{S2}$, MIL53(Al)$_{S3}$,MIL53(Al)$_{S4}$ and MIL53(Al)$_{S5}$.

was indicated in Fig. 2. The system consists of gas flow controllers (Aalborg DFC), valves (V1, V2, and V3), oven (Binder ED 53), zero length column containing MIL-53(Al) adsorbent, soap bubble meter and mass spectrometer (MS, Hiden HPR 20). Water vapor trap (Agilent) was placed before the mass flow controllers to reduce detroit effect of water vapor on gas adsorption. The ZLC cell consists of a small amount of MIL-53(Al) powder sandwiched between two porous sintered discs (Alltech) within 1/8-in Swagelok fitting union. Both ends of the ZLC cell was covered by quartz wool to prevent MIL-53 powders to escape the mass spectrometer. The ZLC cell is located in an oven to adjust the temperature during the experiments.

Initially, the oven is set to the degas temperature and inert Helium gas is sent through the ZLC column by opening the V1 valve. Then, the Helium carrier gas including 10% volume of adsorptive gas (CO_2, CH_4, H_2 or CO) was sent to gas flow controller. The adsorption process was started immediately after opening the V2 valve. Once the stability of adsorption was ensured, desorption process was started by switch off the V3 valve and immediately sending pure Helium gas through the ZLC column.

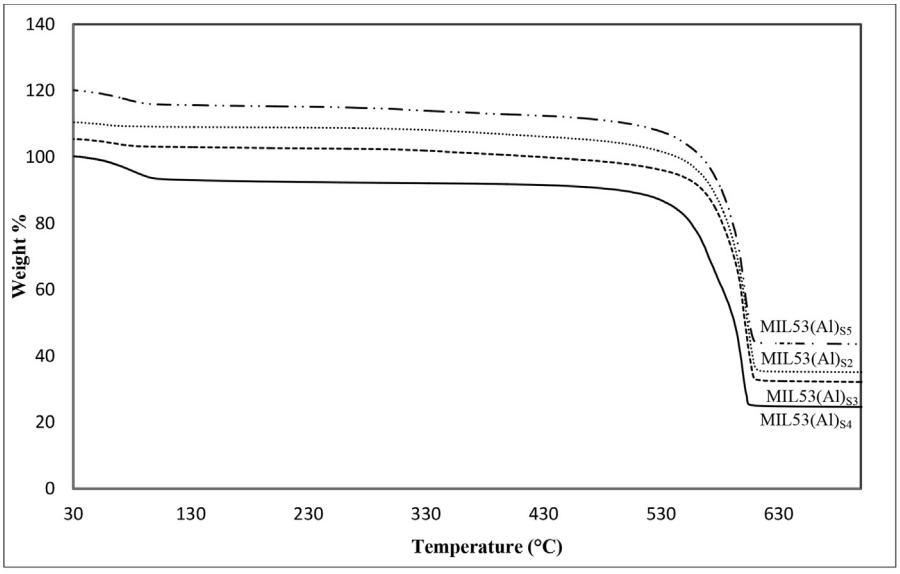

(a)

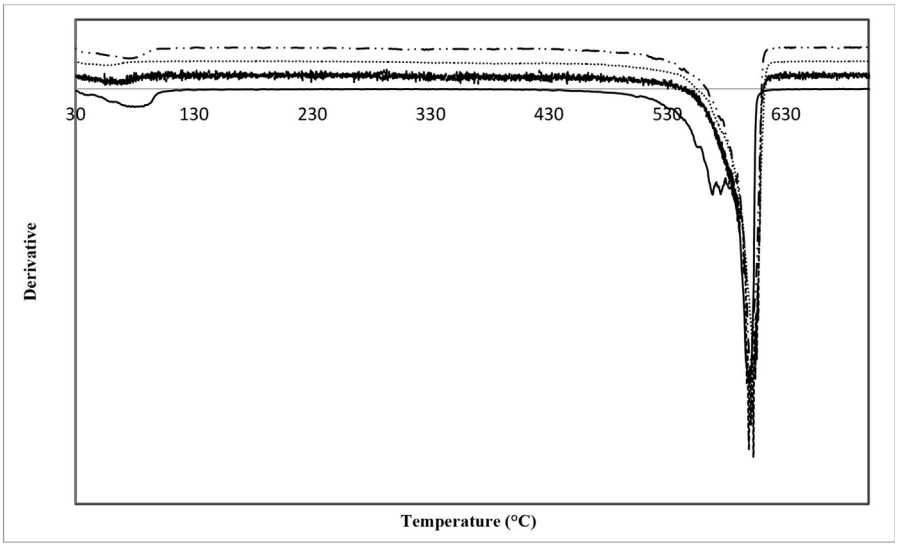

(b)

Fig. 5 – Thermal Gravimetric Analysis (TGA) (a) and derivative TGA (b) of MIL53(Al)$_{S2}$(.....), MIL53(Al)$_{S3}$(( )), MIL53(Al)$_{S4}$( ) and MIL53(Al)$_{S5}$( ).

Results and discussion

The effect of crystallization temperature (T_c) (Code: MIL-53(Al)$_{S2}$ or MIL-53(Al)$_{S3}$ for Tc = 130 °C or 200 °C, respectively); activation temperature (Ta) (Code: MIL-53(Al)$_{S3}$ or MIL-53(Al)$_{S4}$ for 200 °C or 330 °C, respectively) on the crystal structure of aluminum terephthalates (MIL-53(Al)s) were evaluated. Figs. 3–6 shows that SEM, XRD and TGA, FTIR results of MIL-53(Al)s synthesized, respectively. Table 1 also shows the synthesized parameter and their effect on the textural properties. It can be seen from the SEM images that the crystal structure of MIL-53(Al)s constitutes of uneven particles (Fig. 3). From the X-ray diagrams (Fig. 4), the characteristic peaks of MIL-53(Al)s ($2\theta = 8.45°$, 12°, 14.7° and 17.2°) was observed. The XRD patterns obviously demonstrated that the MIL-53(Al)$_{S2}$, MIL-53(Al)$_{S3}$ and MIL-53(Al)$_{S5}$, are well crystalline. Lui et al. studies depending on the synthesis parameter (solvent and temperature used in crystallization step) large and narrow pores form of the MIL-53(Al) can be produced. According the related study, after activation, especially the peaks at $2\theta = 8°$ and $2\theta = 12.5°$ represent the large pore form and narrow pore of the MIL-53(Al)s, respectively. The activation at 330 °C make the structure of MIL-53(Al)$_{S4}$ as narrow pore. On the other hand the crystallization at 130 °C or 200 °C, activation at 130 °C or 200 °C and the purification solvent DMF and or MetOH make MIL-53(Al)s are large-pore form and narrow–pore form.

As seen from Fig. 5, the MIL-53(Al)s were decomposed to amorphous Al_2O_3 at 550 °C. The weight loss in range of 80–130 °C and 568 °C for MIL-53 (Al)$_{S4}$ shows that the thermal activation at 330 °C has negative effect on the crystal structure as supported by XRD pattern. The low intensity shoulder at 3700 cm^{-1} near the broad band is attributed to OH groups in weak hydrogen bonding due to the H_2O in the FTIR spectrum (Fig. 6). The sharp and distinct peaks in the range of 1505–1608 cm^{-1} and 1420-1442 cm^{-1} are corresponded to asymmetric and symmetric stretching modes of $-COO^-$ groups bonded with Aluminums [16]. As a result of FTIR spectrum DMF is into structure when DMF/MetOH was used instead of MetOH to remove the unreacted BDC in the purification step. Textural properties of the MIL-53(Al) shows that the increasing of crystallization temperature from 130 °C to 200 °C decrease the surface area; the increasing of the activation temperature from 200 °C to 330 °C did not change specific surface area considerable but the high temperature increased the external surface area; the highest micropore area was belong to MIL-53(Al)$_{S5}$ purified with MetOH only (Table 1).

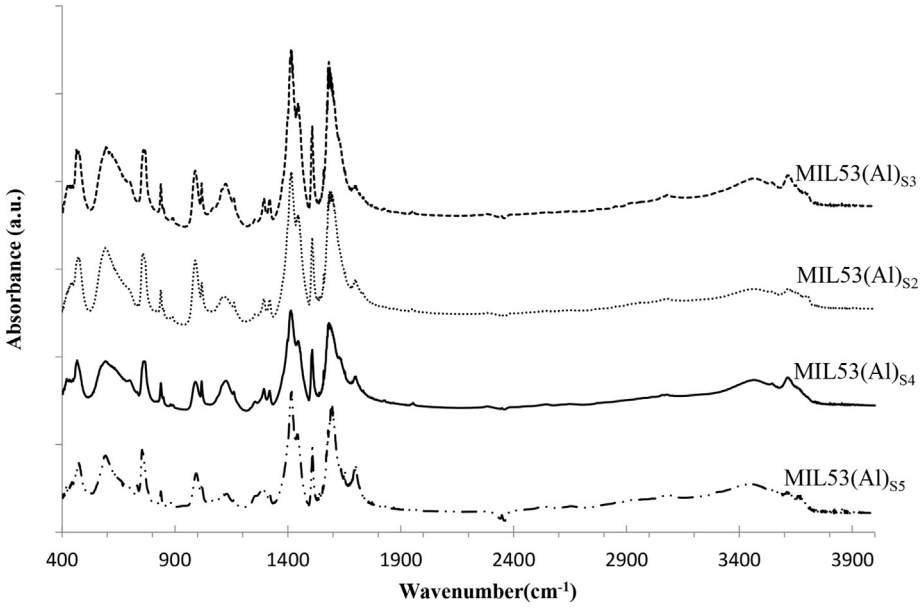

Fig. 6 – FTIR spectra of MIL53(Al)$_{S2}$, MIL53(Al)$_{S3}$, MIL53(Al)$_{S4}$ and MIL53(Al)$_{S5}$.

Table 1 – Synthesis Conditions and textural properties of the Al-TPAs.

Code	Crystallization T_c(°C)/t(h)	Purification Solvent	Activation T_a(°C)/t(h)	A_{Lang} (m2/g)	A_{BET} (m2/g)	A_{micro} (m^2/g)
MIL-53(Al)$_{S2}$	130/72	DMF/MetOH	200/72	1848	1245	925
MIL-53(Al)$_{S3}$	200/72	DMF/MetOH	200/72	1303	883	751
MIL-53(Al)$_{S4}$	130/72	DMF/MetOH	330/72	1678	1111	595
MIL-53(Al)$_{S5}$	130/72	MetOH	130/72	1330	1270	980

A_{Lang}, A_{BET}:Specific surface area calculated from Langmuir, BET models.
A_{micro}: micropore surface ares calculated from t-plot.

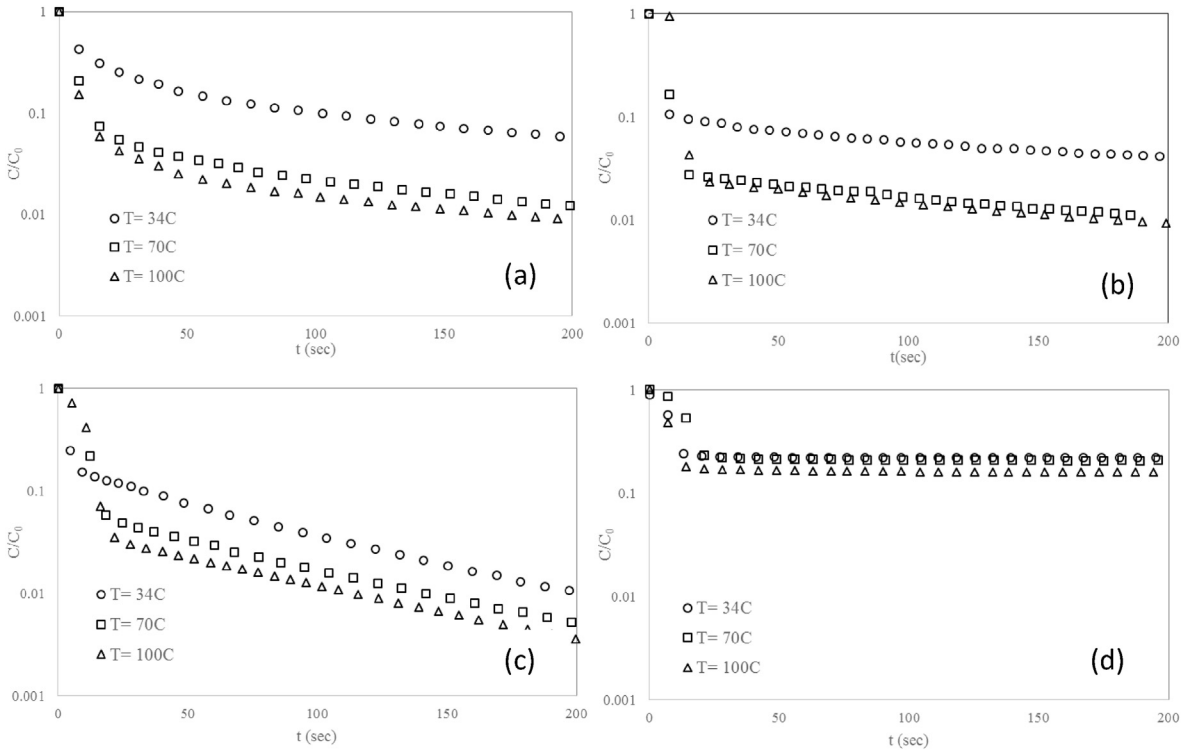

Fig. 7 – The effect of temperature on the ZLC response curves of a) CO_2 b) CH_4 c) H_2 d) CO with 168 mL/min flow rate.

MIL-53(Al)s have been successfully synthesized via solvothermal synthesis route. The optimized experimental conditions were determined considering the characterization results: MIL-53(Al)s do not contain any trace of unreacted BDC even activating at lower temperature than the volatilization temperature of BDC (300 °C). As a result, $MIL\text{-}53(Al)_{S5}$ was chosen as the adsorbent due to the best crystalline and the highest micropore volume.

Adsorption kinetics studies: zero length column (ZLC)

ZLC experiments are conducted to measure the adsorption kinetics governing the exponential decay, so-called long time asymptote region [20]. ZLC method is an efficient analysis tool allowing to evaluate the existence of external mass transfer resistances and demonstrate whether the processes under kinetic control or equilibrium control. Angi [1,21] justified the ZLC technique can be used for adsorption kinetics of steam methane reformer (SMR) components on $MIL\text{-}53(Al)_{S5}$ considering flow rates (80, 168 and 175 mL/min), temperature (34, 70 and 100 °C) and adsorptive concentration (15% and 28%). In this article only the effect of temperature on the adsorption kinetics of steam methane reformer (SMR) components will be presented. The effect of temperature (34, 70 and 100 °C) on the ZLC response curves of CO_2, CH_4, H_2 and CO gases with 168 mL/min flow rate was illustrated in Fig. 7. Under diffusional condition the response curve data were used to calculate the diffusion coefficient (D_c), K and L parameter of CO, CO_2 CH_4 and H_2 and summarize in Table 2. The particle size (R_p) and volume (V_s) of $MIL\text{-}53(Al)_{S5}$ are 31.5×10^{-4} cm and 5×10^{-3} cm^3. The diffusion coefficient is increased with temperature for all gases. H_2 gas has the

Table 2 – The effect of temperature on the kinetic parameters of CO_2, CH_4, H_2 and CO.

GAS	T(°C)	L	(s^{-1})	D (m^2/s)	KV_s (mL)	$Kx10^{-3}$	ΔH (KJ/mol)	E_a (KJ/mol)
CH_4	34	21.7	0.00051	5.03×10^{-13}	40.4	8.09	−9.71	3.98
	70	68.4	0.00059	5.83×10^{-13}	23.2	4.64		
	100	69	0.00067	6.64×10^{-13}	21.1	4.21		
CO_2	34	10.8	0.00058	5.73×10^{-13}	149.6	30	−29.1	5.04
	70	40	0.00077	7.64×10^{-13}	30.3	6.06		
	100	55	0.00081	8.04×10^{-13}	21	4.19		
H_2	34	14	0.00137	1.36×10^{-12}	48.7	9.75	−16.7	2.00
	70	28.7	0.00150	1.49×10^{-12}	21.7	4.34		
	100	38	0.00157	1.56×10^{-12}	15.6	3.13		
CO	34	8.8	0.00001	1.01×10^{-14}	10,468	2094	−28.2	23.92
	70	9	0.00004	4.02×10^{-14}	2559	511		
	100	12	0.00005	5.03×10^{-14}	1535	307		

Table 3 – Thermophysical properties of gases [14].

Properties	CO_2	CO	CH_4	H_2
Kinematic diameter (Å)	3.3	3.760	3.758	2.89
Polarizability (x 10^{25}/cm^3)	29.11	19.5	25.93	8.042
Dipole moment (x 10^{18}/esu.cm)	0	0.10	0	0
Quadrupole moment (x10^{26}/esu.cm^2)	4.3	2.5	0	0.662

highest diffusivity than others. As seen from Table 3, H_2 gas has the smaller kinematic diameters (2.92 Å) than other SMR off gases. Therefore faster and easier penetrate and diffusion in the MIL-53(Al)$_{S5}$ pores. High polarizability and quadrupole property of CO_2 cause stronger interaction of gases with hydroxyl groups of MIL-53(Al), leading to slower diffusion as compared to H_2 gas. The diffusivity values of CH_4 and CO_2 gas are in the same order of magnitude as their kinetic diameters.

Activation energies of gases, namely energy barrier that must be exceeded during diffusion, were calculated by using Arrhenius equation. The heat of adsorption (ΔH) and activation energy (E) were calculated by using the temperature effect on diffusivity (D_c) and Henry's constant (K) and presented in Table 2. CO gas has the highest Henry's constant value due to high dipole moment (0.1 × 10^{18} esu^{-1} cm^{-1}) as compared to other gases.

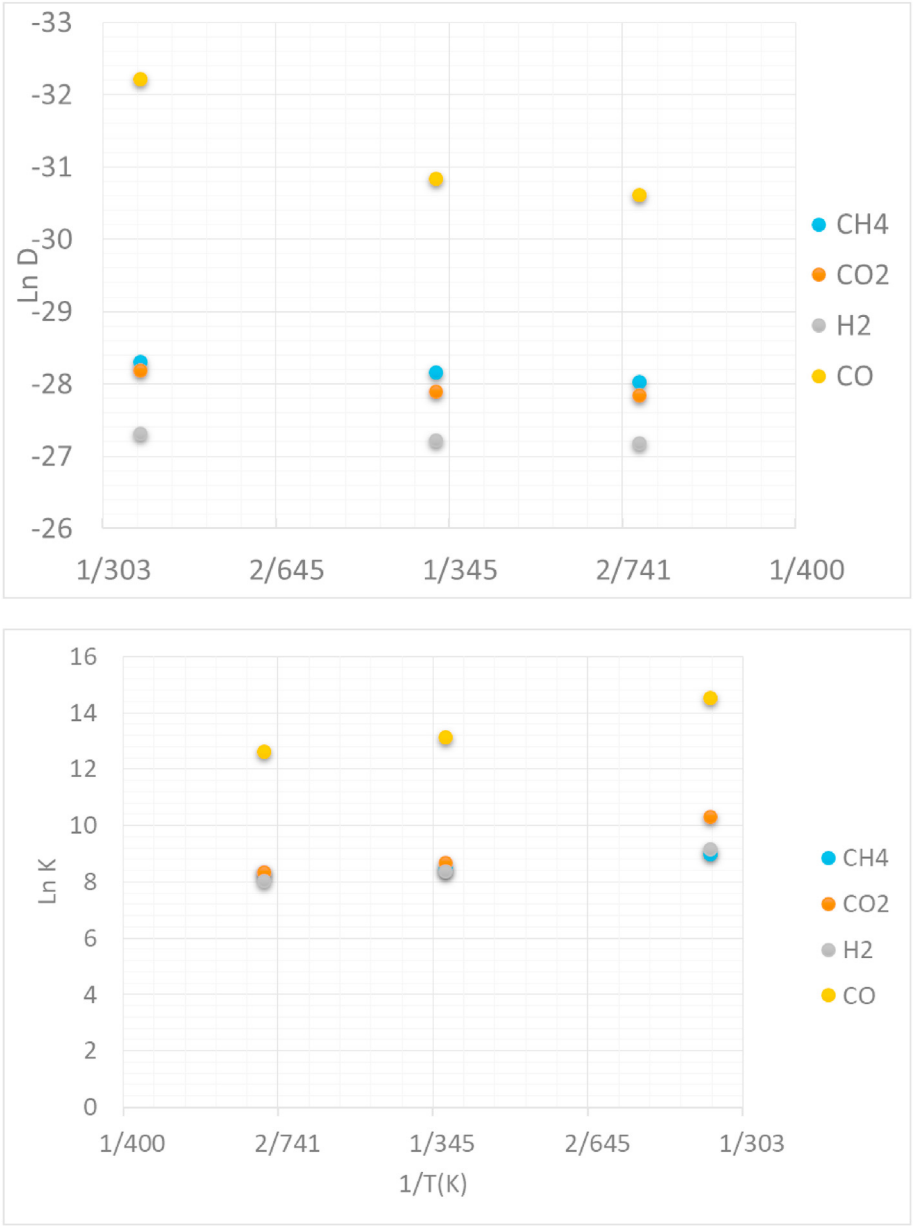

Fig. 8 – Change in the Diffusion coefficient (D) and Henry Constant (K) with reverse temperature.

The heat of adsorption of gases calculated using Van't Hoff equation (Fig. 8). Decreasing of K value with temperature and low values of heat of adsorption demonstrates that physical adsorption was occurred [22]. Heat of adsorption is associated with specific interactions relating with dipole-quadrupole supplemented by polarizability. Having the highest dipole-quadrupole CO_2 gas has highest heat of adsorption value, −29.1 kJ/mol. CO gas has lower heat of adsorption (−28.2 kJ/mol) because of lower quadrupole and polarizability. Having lower dipole-quadrupole and polarizability as compared to CO_2, H_2 has lower heat of adsorption (−16.71 kJ/mol). Heat of adsorption of CH_4 (−9.71 kJ/mol) is lowest since it has no dipole-quadrupole and only polarizability contributes to heat of adsorption. H_2 has the lowest activation energy due to being the smallest gas among the components of SMR off-gases.

Conclusions

In this study, MIL-53(Al) was synthesize and diffusion coefficient of SMR off-gas components were measured via ZLC technique. MIL-53(Al) have been successfully synthesized via a solvothermal synthesis route. With the energy consumption and environmental approach, the MIL-53(Al)$_{SS}$ crystallized at 130 °C, purified with MetOH and activated at 130 °C was chosen as adsorbent. As expected, the diffusion coefficient and activation energy change depending on the kinematic diameter. Activation energy for CO, CO_2, CH_4, and H_2 gases were determined as 23.92, 3.98, 5.05 and 2.00 kJ/mol, respectively. CO gas was more affected by surface characteristics of porous adsorbent due to possessing the highest activation energy. As a result of this study, the solvothermal method can be used to produce narrow and large pore from MIL-53(Al). Adsorption of CO_2, CO, H_2 and CH_4 gases were controlled with electrostatic interaction as observed with ionic adsorbents.

Declaration of competing interest

The authors declare that they have no known competing financial interests or personal relationships that could have appeared to influence the work reported in this paper.

Acknowledgements

The authors would like to thank The Scientific and Technological Research Council of Turkey (project #112M294) and Izmir Institute of Technology, Turkey (project #2016IYTE72) for supporting this study.

REFERENCES

[1] Angı Yaltrık D. Adsorption kinetics of methane reformer off-gases on aluminum based metal-organic frameworks [MSc Thesis]. IZTECH; 2017.

[2] Arstad B, Fjellvåg H, Kongshaug K, Swang O, Blom R. Amine functionalised metal organic frameworks (MOFs) as adsorbents for carbon dioxide. Adsorption 2008;14:755–62.

[3] Brandani F, Ruthven D, Coe CG. Measurement of adsorption equilibrium by the zero length column (ZLC) technique Part 1: single-component systems. Ind Eng Chem Res 2003;42:1451–61.

[4] Loiseau T, Serre C, Huguenard C, Fink G, Taulelle F, Henry M, et al. A rationale for the large breathing of the porous aluminum terephthalate (MIL-53) upon hydration. Chem Eur J 2004;10:1373–82.

[5] Chen XY, Vinh-Thang H, Rodrigue D, Kaliaguine S. Amine-functionalized MIL-53 metal–organic framework in polyimide mixed matrix membranes for CO2/CH4 separation. Ind Eng Chem Res 2012;51:6895–906.

[6] Della Rocca J, Liu D, Lin W. Nanoscale metal–organic frameworks for biomedical imaging and drug delivery. Acc Chem Res 2011;44:957–68.

[7] Drioli E, Barbieri G. Membrane engineering for the treatment of gases. 2nd ed. UK: RSC Publishing; 2011.

[8] Eic M, Ruthven DM. Diffusion of linear paraffins and cyclohexane in NaX and 5A zeolite crystals. Zeolites 1988;8:472–9.

[9] Farha OK, Eryazici I, Jeong NC, Hauser BG, Wilmer CE, Sarjeant AA, et al. Metal–organic framework materials with ultrahigh surface areas: is the sky the limit? J Am Chem Soc 2012;134:15016–21.

[10] Friedrich D, Mangano E, Brandani S. Automatic estimation of kinetic and isotherm parameters from ZLC experiments. Chem Eng Sci 2015;126:616–24.

[11] Brandani S, Cavalcante C, Guimarães A, Ruthven D. Heat effects in ZLC experiments. Adsorption 1998;4:275–85.

[12] Loos JWP, Verheijen PJT, Moulijn JA. Improved estimation of zeolite diffusion coefficients from zero–length column experiments. Chem Eng Sci 2000;55:51–65.

[13] Moulijn JA, Makkee M, Diepen AE. Chemical process technology. 2nd ed. UK: Wiley; 2013.

[14] Mounfield WP, Walton KS. Effect of synthesis solvent on the breathing behavior of MIL-53(Al). J Colloid Interface Sci 2015;447:33–9.

[15] Liu J, Zhang F, Zou X, Yu G, Zhao N, Fan S, et al. Environmentally friendly synthesis of highly hydrophobic and stable MIL-53 MOF nanomaterials. Chem Commun 2013;49:7430–2.

[16] Prausnitz JM, Lichten RN, Azevedo EG. Molecular thermodynamics of fluid-phase equilibria. 2nd ed. USA: Wiley; 1998.

[17] Rostami S, Nakhaei Pour A, Salimi A, Abolghasempour A. Hydrogen adsorption in metal- organic frameworks (MOFs): effects of adsorbent architecture. Int J Hydrogen Energy 2018;43:7072–80.

[18] Ruthven DM. Principles of adsorption and adsorption processes. 1st ed. Canada: Wiley; 1984.

[19] Ruthven DM, Vidoni A. ZLC diffusion measurements: combined effect of surface resistance and internal diffusion. Chem Eng Sci 2012;71:1–4.

[20] Saha D, Deng S. Ammonia adsorption and its effects on framework stability of MOF-5 and MOF-177. J Colloid Interface Sci 2010;348:615–20.

[21] Saha D, Zacharia R, Lafi L, Cossement D, Chahine R. Synthesis, characterization and hydrogen adsorption properties of metal–organic framework Al-TCBPB. Int J Hydrogen Energy 2012;37:5100–7.

[22] Schneemann A, Bon V, Schwedler I, Senkovska I, Kaskel S, Fischer RA. Flexible metal–organic frameworks. Chem Soc Rev 2014;43:6062–96.